Enhanced antitumor efficacy on colon cancer using EGF functionalized PLGA nanoparticles loaded with 5-Fluorouracil and perfluorocarbon

Pingping Wu (wupingpingnano@sina.com)
affiliated cancer hospital of nanjing medical university

Qing Zhou
affiliated cancer hosptial of nanjing medical university

Huayun Zhu
affiliated cancer hosptial of nanjing medical university

Yan Zhuang
affiliated cancer hosptial of nanjing medical university

Jun Bao
affiliated cancer hosptial of nanjing medical university

Research article

Keywords: PLGA nanoparticles, 5-fluorouracil, perfluorocarbon, EGF, hypoxia, colon cancer

Posted Date: November 20th, 2019

DOI: https://doi.org/10.21203/rs.2.17524/v1

Version of Record: A version of this preprint was published at BMC Cancer on April 28th, 2020. See the published version at https://doi.org/10.1186/s12885-020-06803-7.

Abstract

Recurrence and metastasis are the shortcomings of the clinical treatment of colon cancer. Finding an efficacy strategy for the treatment of colon cancer is important. In recent years, PLGA has been shown to have potential as a broad therapeutic drug delivery system. this study aimed to design a dual-loaded nanoparticles drug delivery system to overcome the limitations of chemotherapeutic drugs in colon cancer therapy. We developed epidermal growth factor (EGF) functionalized poly (lactic-co-glycolic acid) (PLGA) nanoparticles (NPs) co-loaded with 5-fluorouracil (5Fu) and perfluorocarbon (PFC) (EGF-PLGA@5Fu/PFC) for target therapy of colon cancer. EGF-PLGA@5Fu /PFC NPs were estimated to have an average size of 200 nm with a 5Fu-loading efficiency of 7.29%. In vitro release profile exhibited a pH-responsive release. CCK-8, Hoechst33342 staining and flow cytometry assays were performed to investigate the functions of EGF-PLGA@5Fu/PFC NPs in SW620 cells. Targeted EGF-PLGA@5Fu/PFC NPs also exhibited higher cellular uptake than non-targeted NPs in colon cancer cells. EGF-PLGA@5Fu/PFC NPs were found to have the best efficiency on cell viability suppression and apoptosis induction in SW620 cells. In xenograft mice, EGF-PLGA@5Fu/PFC NPs had the best suppressive effects on tumor growth compared with 5Fu, PLGA@5Fu and PLGA@5Fu/PFC NPs. The results of histopathological analysis further indicated that EGF-targeted NPs were the most efficient on tumor growth inhibition. Mechanically, the data demonstrated the improved therapeutic outcomes were owing to the fact that PFC could relieve tumor hypoxia via transporting oxygen to the tumor. We creatively constructed a biocompatible nanodrug delivery system and functionalized nanoparticles may provide new potential for selective delivery of chemotherapy drugs to cancers.

Background

Colon cancer is one of the most leading causes of cancer-induced morbidity and mortality worldwide [1]. The clinical therapeutic strategies for colon cancer mainly depend on radiotherapy, chemotherapy and surgery. Nevertheless, there are some disadvantages of these therapeutic modalities. For instance, surgery is usually associated with recurrence and metastasis [2]. Chemotherapy, a predominant strategy for cancer therapy, often produces severe side effects such as poor bioavailability, high system toxicity and multidrug resistance [3]. Therefore, it is of great importance to find an efficacy strategy for the treatment of colon cancer.

In the recent years, great developments have been achieved in the application of nanoparticles for drug delivery due to their advantages such as good biocompatibility and biodegradability [4]. Moreover, specific modification on the large surface of nanoparticles could strengthen the target delivery of chemotherapeutic drugs as well as blood circulation time, ultimately resulting in the excellent treatment outcome [5]. Numerous nanoparticle carriers including cyclodextrins, dendrimers and polymers have been developed in biomedical applications [6–8]. Of these, poly (lactic-co-glycolic acid) (PLGA), a approved polymer by food and drug administration (FDA), has been extensively used as a carrier for drug delivery owing to its ability to encapsulate both hydrophobic and hydrophilic drugs [9]. PLGA have demonstrated their potential as drug delivery systems for a wide range of therapeutic agents. PLGA-based nanoparticles

was delivered to the site of an ischemia/reperfusion (I/R) injury, thereby achieving the anticoagulant and antioxidant ability for vascular therapy [10]. PLGA nanoparticles increased the accumulation of docetaxel at the tumor sites of gastric cancer which led to superior anticancer activities [11]. PLGA nanoparticles was used for sustained and controlled drug delivery with improved bioavailability of hydrophobic compounds such as curcumin [12].

5-fluorouracil (5Fu) is a broadly used chemotherapy drug in various cancers such as colon cancer, liver cancer [13, 14]. As an antimetabolite analogue of pyrimidine, 5Fu inhibited nucleoside metabolism and DNA synthesis, thereby resulting in cell apoptosis [15]. 5Fu also works by participating in survival signal pathways including NF-κB [16]. Nevertheless, the clinical application of 5Fu is often limited due to short half-life, systemic adverse effects, repeated doses to maintain therapeutic levels and non-selective delivery [17]. Hence, it is important to develop an effective delivery carrier for improved utility of 5Fu in cancer therapy.

In the present study, we aimed to design the Epidermal growth factor (EGF) decorated PLGA nanoparticles to enhance the therapeutic effect of colon cancer by co-delivering chemotherapeutic drug 5-fluorouracil (5Fu) and oxygen-transport perfluorocarbon (PFC). The functionalized nanoparticles were fabricated based on PLGA by solvent evaporation method and characterized by morphology, size distribution, *in vitro* stability and release profile. Cell uptake, cytotoxicity and apoptosis assays were employed to evaluate the biological performance of nanoparticles. The distribution, growth suppression and histological changes of nanoparticles were investigated *in vivo* by using SW620 tumor-bearing mice. Finally, the possible mechanism by which nanoparticles exerted the enhanced antitumor effects was explored.

Methods

Preparation of PLGA nanoparticles

PLGA@5Fu/PFC NPs were prepared by a solid-in-oil-in-water (s/o/w) dual emulsion solvent evaporation as described [18]. Briefly, 50 mg of PLGA was dissolved in 2 mL of chloroform containing PFCs (2 mg). 5 mg of 5Fu was dissolved in 0.5 mL of aqueous solvent and then mixed with PLGA solution to generate the s/o primary solution. The emulsion was dispersed in 10 mL of aqueous solvent containing 2% w/v PVA to generate the final s/o/w emulsion. Free PLGA/PVA polymers were separated by centrifugation at 3,000 rpm for 15 min. EGF was modified onto PLGA NPs by N'-ethylcarbodiimide hydrochloride (EDC) method [19].

Characterization of nanoparticles

The shape of EGF-PLGA@5Fu/PFC NPs was examined by transmission electron microscopy (TEM) (Hitachi, Tokyo, Japan). A drop of NPs solution (0.5 mg/mL) was mounted on a carbon-coated copper

grid. The samples were observed at an acceleration voltage of 75 kV. Size distribution and zeta potential were determined by dynamic light scattering (DLS, Zetasizer Nano ZS, Malvern Instruments Ltd, UK).

Drug encapsulation and in vitro release

The encapsulation efficiency of 5Fu in NPs was examined by UV-Vis spectrophotometer (1800, Shimadzu, Kyoto, Japan). Briefly, 1 mg of nanoparticles was dispersed in 1 mL of distilled water for the extraction of 5Fu. The solution was shaken gently for 12 h at 37°C, the obtained filtrates were diluted (1:10) with methanol and measured at λmax = 266 nm. The encapsulation efficiency and loading efficiency were calculated by below equations:

[Due to technical limitations, the formulas could not be displayed here. Please see the supplementary files to access the formulas.]

The release profile of 5Fu from NPs was accessed at different pH values (5.0 or 7.4). 10 mg of NPs were dispersed in 10 mL PBS, then transferred into dialysis bag and placed into 50 mL media with stirring at 37°C. At predetermined time points, 2 mL of release medium was taken out and the equal volume fresh medium was added. The amount of 5Fu released was detected by UV-Vis spectrophotometer.

Cell lines and culture

Human colorectal cancer cell line SW620 was obtained from Chinese Academy of Science (Shanghai, China). SW620 cells were maintained in Dulbecco's Modified Eagle Medium (DMEM) supplemented with 10% fetal bovine serum (FBS). Cells were routinely cultured in a humidified cell incubator with 5% CO_2 at 37°C.

In vitro cell uptake

SW620 cells were cultured in 12-well plate at a density of 2×10^4 cells/well. After 24 h, fresh DMEM medium with Cy5-labeled NPs (EGF-PLGA@5Fu/PFC and PLGA@5Fu/PFC) were added and cultured at 37°C for 2 h, 4 h and 6 h. Cells were washed with PBS, fixed with 4% paraformaldehyde and deposited with DAPI. At last, cells were observed by confocal laser scanning microscope (CLSM).

Cell cytotoxicity

SW620 cells were cultured in 96-well plate at a density of 2×10^3 cells/well. After 24 h, different formulations of NPs were added into cells and cultured for 48 h at 37°C. Then, 10 μL of CCK-8 was added to each well and incubated for another 4 h. The optical density was measured at 450 nm by a microplate reader (BioRad, Hercules, CA, USA).

Hoechst 33342 staining

SW620 cells (1×10^4 cells/well) were seeded in 24-well plate, and treated with different formulations of NPs for 48 h. Then, cells were washed with PBS for three times and stained with Hoechst (2 μg/mL) for 20 min at room temperature. Stained cells were observed under a fluorescent microscope (Nikon TE2000; Nikon Corporation, Tokyo, Japan) (magnification, ×100).

Cell apoptosis

SW620 cells (1×10^5 cells/well) were cultured in 6-well plate with different formulations of NPs for 48 h. Then, cells were washed with PBS twice, suspended in staining buffer containing propidium iodide (PI) (1 μg/mL) and annexin V-FITC (0.025 μg/mL) for 15 min at room temperature. Apoptotic cells were evaluated by using FACScalibur flow cytometer (BD Bioscience, Franklin lakes, NJ).

Animal model establishment

Female BALB/c mice (6-8 weeks, 20-22 g) were obtained from the Animal Laboratory of Nanjing University and were kept in the standard conditions with humidity 50%-60%, temperature 25 ± 2°C, 12-h dark/light cycle and access to free water and food. All the animal experiments were carried out in line with the Guidelines for Care and Use of Laboratory Animals of the University of Science and Technology of China and approved by the Animal Ethics Committee of Nanjing Medical University.

SW620 cells (3×10^6) were resuspended in 100 μL PBS and injected into the right flank of mice. When the average tumor volume reached about 100 mm^3, mice were assigned into 6 groups (n=8) and administrated with saline, blank NPs (100 mg/kg), 5Fu (8 mg/kg), PLGA@5Fu (8 mg/kg of 5Fu), PLGA@5Fu&PFC (8 mg/kg of 5Fu) and EGF-PLGA@5FU&PFC (8 mg/kg of 5Fu) every two days. The tumor size was measured and volume was calculated as follows: volume (cm^3) = Length (L) × $Width^2$ (W^2)/2. At the end, mice were sacrificed by intraperitoneal injection of sodium pentobarbital (100 mg/kg), tumor and major organs were isolated for further experiments.

Ex vivo fluorescence imaging

After 24 h of injection, mice were sacrificed and the biodistribution of different formulations of drugs in the tumor and major organs was determined using a fluorescence imaging system.

Histological analysis

Tissues from the mice were fixed in 10% formalin, embedded in paraffin and cut into 5-μm sections. The sections were stained with haematoxylin and eosin (H&E) to evaluate the histological changes of tumor and major organs. For TUNEL assay, tumor tissues were stained with an in situ apoptosis detection kit (Thermo Fisher Scientific) according to the manufacturer's directions. For immunohistochemical staining (IHC), tumor tissues were incubated with primary antibody against Ki-67 (ab15580, Abcam). Images for H&E and IHC were obtained by a light microscope, images for TdT-mediated dUTP nick end labeling (TUNEL) were acquired by a fluorescent microscope.

Immunofluorescence staining

At the end, mice were intravenous injected with pimonidazole at the dose of 60 mg/kg for hypoxia staining. After 90 min, tumors were collected, imbedded and cut into 8-μm section. Subsequently, the tumor tissue was incubated with the primary antibody against pimonidazole (1:200, Hpoxyprobe-1 Plus Kit, Hypoxyprobe, Burlington) at 4°C overnight, followed by incubation with Alexa Fluo® 488 conjugated goat-anti-mouse antibody (1:500, ab150113, Abcam) for 1 h at 37°C. The nuclei were counterstained with DAPI for 3 min. Finally, images were captured under fluorescence microscope (magnification, ×200).

Statistical analysis

All data was analyzed by GraphPad Prism 5.0 and presented as mean ± standard deviation. One way ANOVA analysis followed by Tukey's post hoc test was used to compare the difference between multiple groups. A $p<0.05$ was considered statistically significant.

Results

Characterization of nanoparticles

To prepare EGF-PLGA@5Fu/PFC NPs, 5Fu was encapsulated in PLGA polymer via double emulsification solvent evaporation method. The morphology of 5Fu loaded PLGA NPs was observed under TEM (Figure 1A), showing the monodispersive and spherical nature with a size around 200 nm. The results of DLS confirmed the average diameter of EGF-PLGA@5Fu/PFC NPs was 200 ± 10.84 nm, revealing the

formation of nanosystems with a narrow distribution (Figure 1B). The zeta potential analysis suggested that EGF-PLGA@5Fu/PFC NPs exhibited a negative surface charge of -23.7 ± 1.4 mV. In addition, the encapsulation efficiency and drug loading efficiency were found to be 81.6 ± 5.7% and 7.29 ± 0.14%, respectively. The release profile of 5Fu loaded PLGA NPs was determined at different pH values (5.0 or 7.4), and the release behavior displayed a biphasic drug release pattern consisting of initial accelerated release followed by a sustained release over 7 days. As shown in Figure 1C, the accumulated release amount of 5Fu from EGF-PLGA@5Fu/PFC NPs reached about 45% within 6 h and 80% within 7 days at pH 5.0. In comparison, EGF-PLGA@5Fu/PFC NPs exhibited a slow drug release at pH 7.4, indicating that EGF-PLGA@5Fu/PFC NPs could achieve the rapid 5Fu release in acid condition of cancer cells.

In vitro cellular uptake

The presence of surface EGF endows EGF-PLGA@5Fu/PFC NPs with intensive interactions to EGFR, prompting them anchoring to cancer cells that highly express EGFR. In order to check the targeting capability of EGF-PLGA@5Fu/PFC NPs, SW620 cells were incubated with Cy5 labeled NPs for 2 h, 4 h and 6 h after pretreated or unpretreated with free EGF. The cellular uptake of EGF-PLGA@5Fu/PFC NPs was determined by CLSM. As depicted in Figure 2, the fluorescence intensity of unpretreated cells incubated with EGF-PLGA@5Fu/PFC NPs was stronger than that of non-targeted NPs (PLGA@5Fu/PFC), and the uptake increased in a time-dependent manner, suggesting higher adsorption of EGF-PLGA@5Fu/PFC NPs to colon cancer cells. To further investigate the role of EGFR on cell surface in binding, free EGF competition study was performed by pretreating SW620 cells with high concentration of EGF (100 μg/mL) for 1 day. The results showed that EGF distinctively decreased the uptake of EGF-PLGA@5Fu/PFC NPs in SW620 cells compared with unpretreated cells as evidenced by the relatively weaker fluorescence intensity, verifying that the binding efficiency of EGF-PLGA@5Fu/PFC NPs to cancer cells was positively associated with EGFR expression level. The results identified that EGF-PLGA@5Fu/PFC NPs could effectively increase the cellular uptake in EGF receptor-mediated endocytosis.

In vitro cell cytotoxicity and apoptosis

To investigate the *in vitro* antitumor capability of 5Fu loaded NPs, SW620 cells were cultured and incubated with blank NPs, 5Fu, PLGA@5Fu NPs, PLGA@5Fu/PFC NPs and EGF-PLGA@5Fu/PFC NPs, respectively. As observed in Figure 3A, CCK-8 results indicated free 5Fu, PLGA@5Fu NPs, PLGA@5Fu/PFC NPs and EGF-PLGA@5Fu/PFC NPs had inhibitory effects on cellular proliferation of colon cancer cells in a concentration dependent manner. In addition, EGF-PLGA@5Fu/PFC NPs exhibited the obvious cellular proliferation suppression to SW620 cells than PLGA@5Fu/PFC NPs, PLGA@5Fu NPs and free 5Fu. In the meanwhile, EGF-PLGA had no remarkable cytotoxicity toward colon cancer cells.

In response to antitumor agents, cancer cells usually experience apoptosis. To explore the cell apoptosis induced by 5Fu loaded NPs, cell were stained with Hoechst33342 to observe apoptotic morphology. As illustrated in Figure 3B, cells treated with free 5Fu, PLGA@5Fu NPs, PLGA@5Fu/PFC NPs or EGF-PLGA@5Fu/PFC NPs exhibited apoptotic features at different degrees, such as nuclei fragmentation and chromatin condensation, and cells treated with EGF-PLGA@5Fu/PFC NPs displayed the significantly

obvious apoptotic features. Meanwhile, cells treated with blank NPs seemed to have little impact on cell morphology.

Further studies on antitumor capability were achieved by evaluating the total apoptosis of SW620 cells in the presence of NPs using flow cytometry. Figure 3C suggested that treatment with EGF-PLGA@5Fu/PFC NPs (34%) caused the highest apoptosis of cancer cells than those with free 5Fu (15.4%), PLGA@5Fu NPs (26%), PLGA@5Fu/PFC NPs (26.5%). In consistent with the cellular uptake assay, these results demonstrated that EGF in EGF-PLGA@5Fu/PFC NPs would be beneficial to enhancing cell viability suppressive effects via anchoring 5Fu loaded NPs on SW620 cells, thereby promoting the accumulation of 5Fu in tumor cells.

In vivo antitumor effects of PLGA nanoparticles

To investigate the *in vivo* distribution of 5Fu loaded NPs, tumor-bearing mice were injected with Cy5-labeled NPs via tail vein, followed by collecting tumors and the major organs for ex vivo imaging. Figure 4A indicated that mice treated with EGF-PLGA@5Fu/PFC NPs exhibited obviously stronger fluorescence signal at tumor site than that with PLGA@5Fu/PFC NPs, which might be attributed to the effective tumor accumulation ability of EGF-targeted NPs in tumors via ligand-receptor mediated endocytosis. To be mentioned, the relatively recognizable fluorescence signals also appeared in the liver due to the cellular uptake by endothelial cells and phagocytic cells. The findings suggested that EGF-targeting NPs could promote the accumulation at tumor sites preferentially.

To assess the chemotherapeutic effects of 5Fu loaded NPs *in vivo*, the tumor-bearing mice were administrated with different formulations. From Figure 4B, it could be observed that the growth rate of tumor size in mice treated with EGF-PLGA@5Fu/PFC NPs was significantly lower than that in groups treated with free 5Fu, PLGA@5Fu NPs and PLGA@5Fu/PFC NPs, although the tumor growth rate of groups treated with different formulations of 5Fu had downward trend. It could be concluded that EGF modified NPs exerted an important role in tumor targeting so that drugs were more accumulated in the tumor site, resulting in a better therapeutic effect. Mice treated with saline and blank NPs had the fastest tumor growth rate. Meanwhile, tumor volume and weight after injection for 20 days also demonstrated that EGF-PLGA@5Fu/PFC NPs had the best therapeutic effect (Figure 4C and D).

Histological analysis

Next, the histological analysis was performed to test the *in vivo* effects on the major organs and tumor tissue by H&E staining, TUNEL and IHC. As shown in Figure 5A-C, saline treated group showed normal tumor cells, whereas different drug formulations treated group displayed various degrees of tumor necrosis. In comparison, EGF-targeted NPs exhibited the highest tumor necrosis. Besides, higher hepatic toxicity was observed in free 5Fu group, which was due to the most common side effect of chemotherapeutic drugs caused by first-pass effect. The similar results of tumor inhibition induced by different drug formulations were also confirmed by TUNEL and IHC assays.

Motivated by the above results that PLGA@5Fu/PFC NPs showed more effective on tumor growth than PLGA@5Fu NPs, we speculated that PFC could modulate tumor hypoxia to achieve the improved therapeutic outcomes. To identify the hypothesis, pimonidazole, an injectable hypoxia-specific probe, was used to trace the hypoxia state of tumor. As shown in Figure 6, immunofluorescence imaging manifested that EGF-PLGA@5Fu/PFC NPs treatment showed significantly weaken pimonidazole green fluorescence compared with the control group, revealing the decreased tumor hypoxia, which was consistent with previous publication that PFC could transport oxygen to tumor [20]. Therefore, it could be concluded that the superior effect achieved by PFC-based NPs was partially attributed to the improved tumor oxygenation.

Discussion

Due to some obstacles including high toxicity, repeated dosage and non-specific accumulation, monotherapy by 5Fu usually cannot reach satisfactory antitumor effects in colon cancer treatment. In this study, we developed EGF-modified PLGA NPs co-loaded with 5Fu and PFC to overcome the limitations. The data indicated that the synergetic antitumor efficacy of EGF-PLGA@5Fu/PFC NPs was better than that of other combination in suppressing cell proliferation and promoting cell apoptosis *in vitro* and attenuating tumor growth *in vivo.* Moreover, no obvious lesion in major organs was found after treatment with NPs, demonstrating the safety of NPs.

To improve the efficacy of chemotherapeutic drugs in cancer treatment, employing NPs with targeted delivery property is a promising method [21]. EGF is a commonly used binding agent for EGF receptor-overexpressing solid tumors including colon cancer [22]. Colon cancer cells SW620 were chosen as EGF receptor overexpressing tumor cells to investigate the target ability of EGF-PLGA@5Fu/PFC NPs. The results showed increased cellular uptake of EGF-PLGA@5Fu/PFC NPs to colon cells by binding to EGF receptors on the cell surface. Using EGF receptor-targeted PLGA NPs conjugated with curcumin, more efficient celluar uptake was observed in MCF–7 cells [23]. Similarly, it was also demonstrated that EGF receptor-mediated cellular uptake of silica NPs loaded with zinc phthalocyanime was remarkably greater for pancreatic cancer cells [24]. Thus, in line with previous publications, EGF decoration could promote the cellular uptake of NPs to tumors overexpressed EGF receptors.

Co-delivery of multiple drugs by nanocarriers usually presents an outstanding strategy than monotherapeutic agents through multiple pathways. Dual-loaded PLGA NPs encapsulating doxorubicin and curcumin had higher antitumor effects against breast cancer because curcumin could protect drugs from being excluded by P-glycoprotein (P-gp) [25]. A self-assembled nanosystem co-loaded with trichosanthin (TCS) protein and albendazole (ABZ) exhibited great antitumor effect through overcoming multidrug resistance [26]. It is well established that tumor hypoxia could cause chemotherapy resistance [27]. PFC, commonly applied as oxygen carrier in clinical use, has been reported to have the capability of delivering oxygen to tumor environments [28]. In our study, dual-loaded PLGA NPs encapsulating 5FU and PFC had the combinative antitumor effects on colon cancer, likely owing to that PFC in the tumor altered

the diffusion status of the oxygen in tumor tissue. This was in agreement with the existing researches that PFC had great potential for enhancing intratumoral hypoxia [29, 30].

Conclusions

In conclusion, we successfully constructed a biocompatible nanodrug delivery system that could selectively accumulate in tumor via ligand-targeting interactions and overcome hypoxia-induced chemotherapy resistance via increasing the tumor local oxygen level, thereby resulting in the improved therapy effects.

Abbreviations

PLGA: poly (lactic-co-glycolic acid); FDA: food and drug administration; I/R: ischemia/reperfusion: 5Fu: 5-fluorouracil; EGF: epidermal growth factor; PFC: perfluorocarbon; EDC: N'-ethylcarbodiimide hydrochloride; TEM: transmission electron microscopy; DLS: dynamic light scattering; DMEM: Dulbecco's Modified Eagle Medium; FBS: fetal bovine serum; CLSM: confocal laser scanning microscope; H&E: haematoxylin and eosin; IHC: immunohistochemical staining; TUNEL: TdT-mediated dUTP nick end labeling; NPs: nanoparticles; TCS: trichosanthin; ABZ: albendazole; P-gp: P-glycoprotein

Declarations

Acknowledgements

Not applicable.

Funding

This project was supported by the National Natural Science Youth Foundation of China (No. 81601604), the Natural Science Youth Foundation of Jiangsu (No. BK20161070), the Fifteenth Batch High-level Talents Project of "Six Talent Peaks" in Jiangsu Province (No.WSW-049) and the talents program of Jiangsu Cancer Hospital (No. YC201809).

Availability of data and materials

All data generated or analysed during this study are included in this published article.

Authors' contributions

P.W., Q.A., Y.Z. and H.Z. performed the experiment and/or performed data analysis. P.W., Q.A. prepared the manuscript. J.B. contributed to the study design. All authors read and approved the final manuscript.

Ethical approval and consent to participate

Not applicable.

Consent to publication

Not applicable.

Competing interest

There are no known competing of interest associated with this publication.

References

1. Torre LA, Bray F, Siegel RL, Ferlay J, Lortet-Tieulent J, Jemal A. Global cancer statistics, 2012. CA Cancer J Clin. 2015; 65(2):87-108.
2. Yaffee P, Osipov A, Tan C, Tuli R, Hendifar A. Review of systemic therapies for locally advanced and metastatic rectal cancer. J Gastrointest Oncol. 2015; 6(2):185-200.
3. Din FU, Aman W, Ullah I, Qureshi OS, Mustapha O, Shafique S, et al. Effective use of nanocarriers as drug delivery systems for the treatment of selected tumors. Int J Nanomedicine. 2017; 12:7291-7309.
4. Yang S, Gao H. Nanoparticles for modulating tumor microenvironment to improve drug delivery and tumor therapy. Pharmacol Res. 2017; 126:97-108.
5. Jeetah R, Bhaw-Luximon A, Jhurry D. Nanopharmaceutics: phytochemical-based controlled or sustained drug-delivery systems for cancer treatment. J Biomed Nanotechnol. 2014; 10(9):1810-40.
6. Santos CIAV, Ribeiro ACF, Esteso MA. Drug Delivery Systems: Study of Inclusion Complex Formation between Methylxanthines and Cyclodextrins and Their Thermodynamic and Transport Properties. Biomolecules. 2019; 9(5).
7. Palmerston Mendes L, Pan J, Torchilin VP. Dendrimers as Nanocarriers for Nucleic Acid and Drug Delivery in Cancer Therapy. Molecules. 2017; 22(9).
8. Grigoras AG. Polymer-lipid hybrid systems used as carriers for insulin delivery. Nanomedicine. 2017; 13(8):2425-2437.
9. Rezvantalab S, Drude NI, Moraveji MK, Güvener N, Koons EK, Shi Y, et al. PLGA-Based Nanoparticles in Cancer Treatment. Front Pharmacol. 2018; 9:1260.

10. Lee PC, Zan BS, Chen LT, Chung TW. Multifunctional PLGA-based nanoparticles as a controlled release drug delivery system for antioxidant and anticoagulant therapy. Int J Nanomedicine. 2019; 14:1533-1549.
11. Cai J, Qian K, Zuo X, Yue W, Bian Y, Yang J, et al. PLGA nanoparticle-based docetaxel/LY294002 drug delivery system enhances antitumor activities against gastric cancer. J Biomater Appl. 2019; 33(10):1394-1406.
12. Xie X, Tao Q, Zou Y, Zhang F, Guo M, Wang Y, et al. PLGA nanoparticles improve the oral bioavailability of curcumin in rats: characterizations and mechanisms. J Agric Food Chem. 2011; 59(17):9280-9.
13. Ni W, Li Z, Liu Z, Ji Y, Wu L, Sun S, et al. Dual-Targeting Nanoparticles: Codelivery of Curcumin and 5-Fluorouracil for Synergistic Treatment of Hepatocarcinoma. J Pharm Sci. 2019;108(3):1284-1295.
14. Sharma A, Kaur A, Jain UK, Chandra R, Madan J. Stealth recombinant human serum albumin nanoparticles conjugating 5-fluorouracil augmented drug delivery and cytotoxicity in human colon cancer, HT-29 cells. Colloids Surf B Biointerfaces. 2017;155:200-208.
15. Astolfi P, Giorgini E, Gambini V, Rossi B, Vaccari L, Vita F, et al. Lyotropic Liquid-Crystalline Nanosystems as Drug Delivery Agents for 5-Fluorouracil: Structure and Cytotoxicity. Langmuir. 2017;33(43):12369-12378.
16. Hiremath CG, Kariduraganavar MY, Hiremath MB. Synergistic delivery of 5-fluorouracil and curcumin using human serum albumin-coated iron oxide nanoparticles by folic acid targeting. Prog Biomater. 2018;7(4):297-306.
17. Handali S, Moghimipour E, Rezaei M, Ramezani Z, Kouchak M, Amini M, et al. A novel 5-Fluorouracil targeted delivery to colon cancer using folic acid conjugated liposomes. Biomed Pharmacother. 2018;108:1259-1273.
18. Haggag YA, Matchett KB, Dakir el-H, Buchanan P, Osman MA, Elgizawy SA, et al. Nano-encapsulation of a novel anti-Ran-GTPase peptide for blockade of regulator of chromosome condensation 1 (RCC1) function in MDA-MB-231 breast cancer cells. Int J Pharm. 2017; 521(1-2):40-53.
19. Li K, Liu Y, Zhang S, Xu Y, Jiang J, Yin F, et al. Folate receptor-targeted ultrasonic PFOB nanoparticles: Synthesis, characterization and application in tumor-targeted imaging. Int J Mol Med. 2017; 39(6):1505-1515.
20. Lowe KC. Synthetic oxygen transport fluids based on perfluorochemicals: applications in medicine and biology. Vox Sang. 1991;60(3):129-40.
21. Hu CM, Aryal S, Zhang L. Nanoparticle-assisted combination therapies for effective cancer treatment. Ther Deliv. 2010;1(2):323-34.
22. Yun S, Kwak Y, Nam SK, Seo AN, Oh HK, Kim DW, et al. Ligand-Independent Epidermal Growth Factor Receptor Overexpression Correlates with Poor Prognosis in Colorectal Cancer. Cancer Res Treat. 2018;50(4):1351-1361.
23. Jin H, Pi J, Zhao Y, Jiang J, Li T, Zeng X, et al. EGFR-targeting PLGA-PEG nanoparticles as a curcumin delivery system for breast cancer therapy. Nanoscale. 2017;9(42):16365-16374.

24. Er Ö, Colak SG, Ocakoglu K, Ince M, Bresolí-Obach R, Mora M, et al. Selective Photokilling of Human Pancreatic Cancer Cells Using Cetuximab-Targeted Mesoporous Silica Nanoparticles for Delivery of Zinc Phthalocyanine. Molecules. 2018;23(11).
25. Lv L, Qiu K, Yu X, Chen C, Qin F, Shi Y, et al. Amphiphilic Copolymeric Micelles for Doxorubicin and Curcumin Co-Delivery to Reverse Multidrug Resistance in Breast Cancer. J Biomed Nanotechnol. 2016; 12(5):973-85.
26. Tang Y, Liang J, Wu A, Chen Y, Zhao P, Lin T, et al. Co-Delivery of Trichosanthin and Albendazole by Nano-Self-Assembly for Overcoming Tumor Multidrug-Resistance and Metastasis. ACS Appl Mater Interfaces. 2017; 9(32):26648-26664.
27. Minassian LM, Cotechini T, Huitema E, Graham CH. Hypoxia-Induced Resistance to Chemotherapy in Cancer. Adv Exp Med Biol. 2019;1136:123-139.
28. Ahrens ET, Helfer BM, O'Hanlon CF, Schirda C. Clinical cell therapy imaging using a perfluorocarbon tracer and fluorine-19 MRI. Magn Reson Med. 2014;72(6):1696-701.
29. Wang W, Cheng Y, Yu P, Wang H, Zhang Y, Xu H, et al. Perfluorocarbon regulates the intratumoural environment to enhance hypoxia-based agent efficacy. Nat Commun. 2019;10(1):1580.
30. Xiang Y, Bernards N, Hoang B, Zheng J, Matsuura N. Perfluorocarbon nanodroplets can reoxygenate hypoxic tumors in vivo without carbogen breathing. Nanotheranostics. 2019;3(2):135-144.

Figures

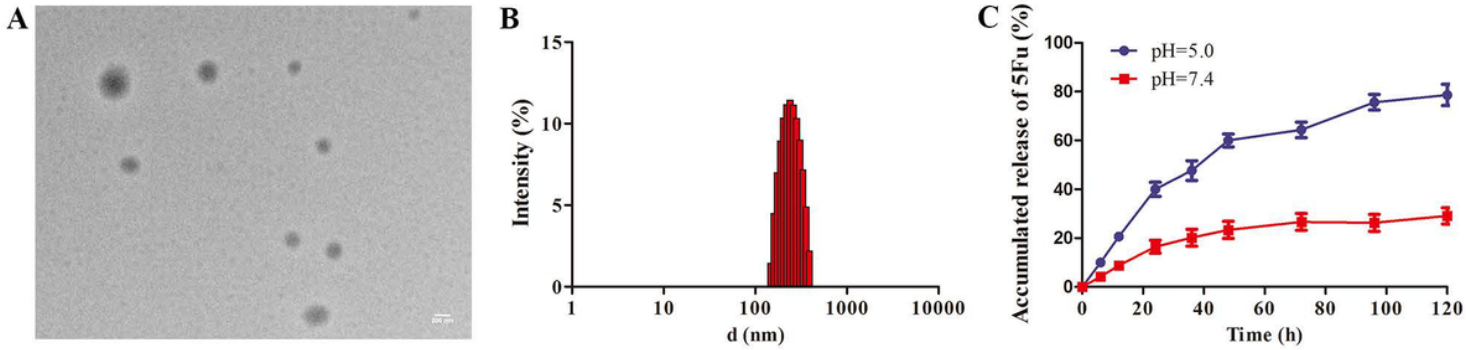

Figure 1

Characterization of EGF-PLGA@5Fu/PFC NPs. (A) The morphology of EGF-PLGA@5Fu/PFC NPs was observed by TEM. (B) Size distribution of EGF-PLGA@5Fu/PFC NPs was detected by DLS. (C) The in vitro release of 5FU from EGF-PLGA@5Fu/PFC NPs at different pH values was monitored by by UV-Vis spectrophotometer.

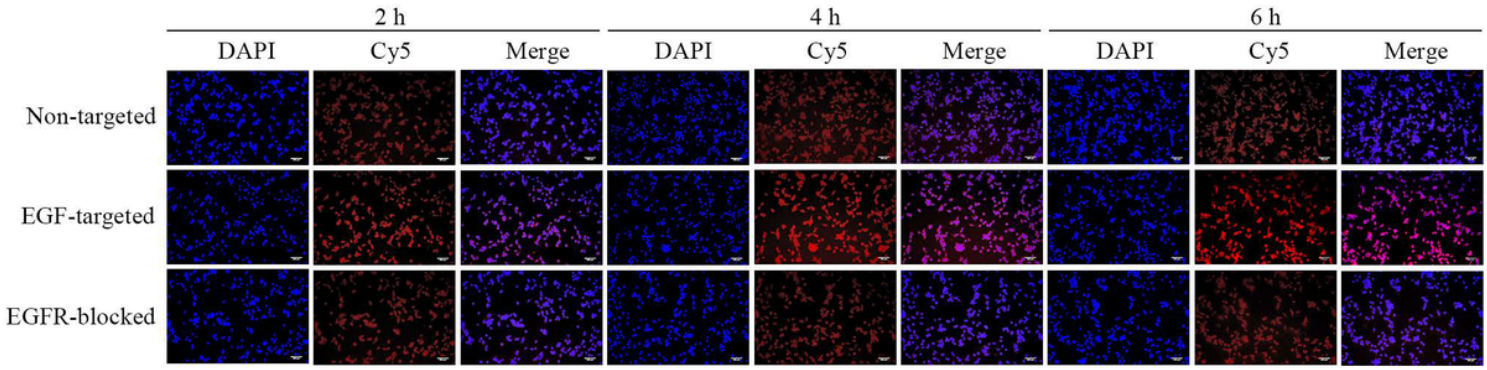

Figure 2

In vitro cellular uptake of EGF-PLGA@5Fu/PFC NPs to SW620 cells was detected by confocal laser scanning microscope (magnification, ×200).

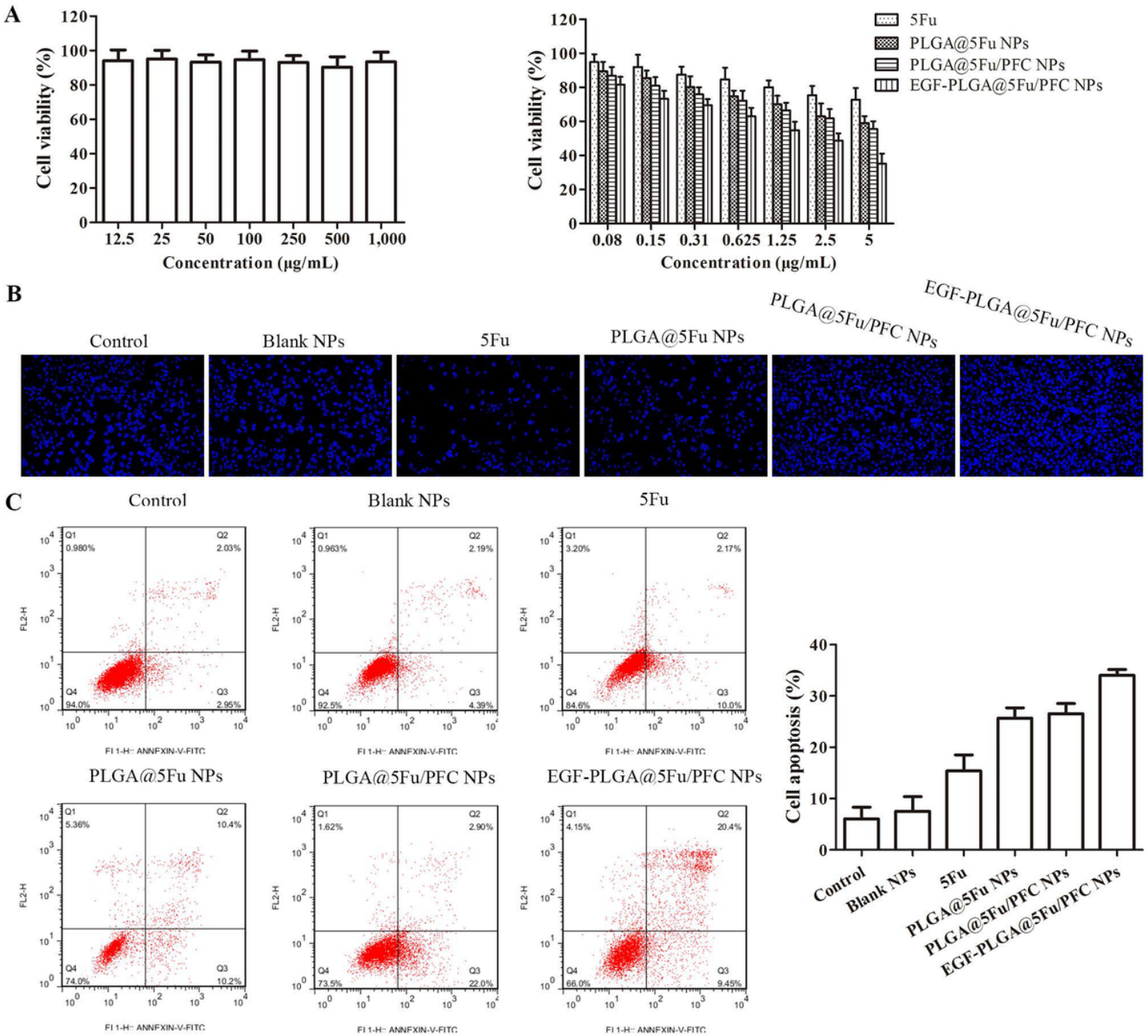

Figure 3

Effects of EGF-PLGA@5Fu/PFC NPs on the proliferation and apoptosis in SW620 cells. (A) Cell viability of SW620 cells was assessed by CCK-8. (B) Cell apoptosis of SW620 cells was evaluated by Hoechst33342 staining (magnification, ×200). (C) Cell apoptosis of SW620 cells was also examined by flow cytometry.

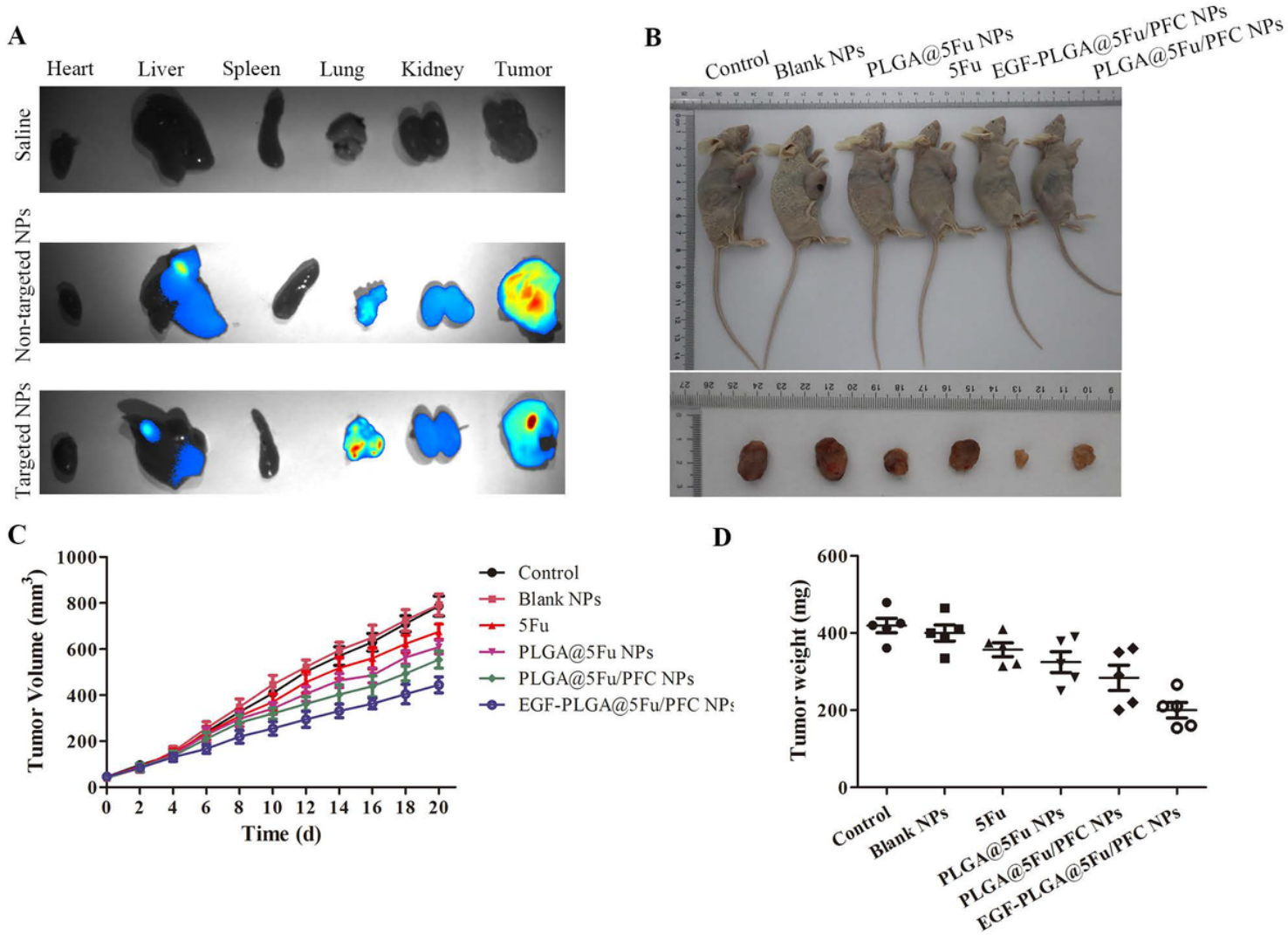

Figure 4

In vivo biodistribution of EGF-PLGA@5Fu/PFC NPs and tumor growth in tumor-bearing mice. (A) The biodistribution of EGF-PLGA@5Fu/PFC NPs in tumor-bearing mice was analyzed by Ex vivo imaging (magnification, ×200). (B) Tumor volume and weight were monitored.

Figure 5

Effect of EGF-PLGA@5Fu/PFC NPs on colon cancer in tumor-bearing mice. Histological analysis of EGF-PLGA@5Fu/PFC NPs was detected by HE (A), TUNEL (B) and IHC (C) assays (magnification, ×200).

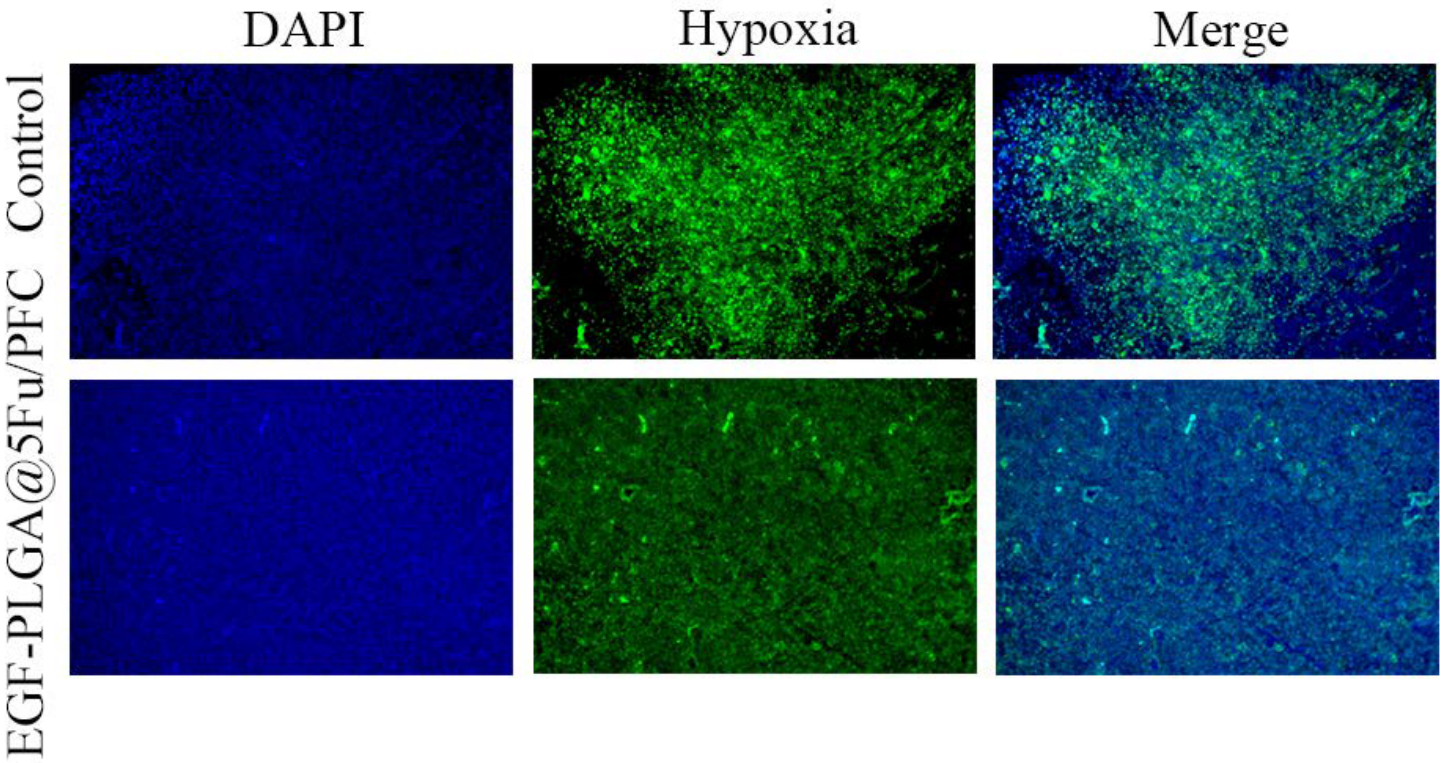

Figure 6

Tumor hypoxia was observed under immunoflurosence microscope (magnification, ×200).

Supplementary Files

This is a list of supplementary files associated with this preprint. Click to download.

- Methodsformulas.docx
- ARRIVEGuidelines.docx